

Electromagnetic force computation with the Eggshell method

F. Henrotte, M. Felden, M. vander Giet and K. Hameyer

Institute of Electrical Machines, Schinkelstraße 4, D-52056 Aachen, Germany
E-mail: fh@iem.rwth-aachen.de

Abstract—In a previous paper, we have proposed a method, called the eggshell method, to compute electromagnetic forces in a finite element (FE) context. This method stems from the rigorous application of the virtual work principle in a mathematical setting where electromagnetic fields are represented by differential forms [6]. The purpose of this paper is to propose an implementation of the eggshell method. The proposed algorithm not only provides the values of the forces but offers also the user the opportunity to perform a number of consistency and accuracy checks, and to investigate more in details the structure of the force field.

Index Terms—Electromagnetic forces, Electromechanical coupling, Maxwell stress tensor, Virtual work principle.

I. INTRODUCTION

In a previous work [9], we have proposed a method to compute electromagnetic forces in a finite element (FE) context. This method, called the **eggshell method**, allows computing both **local** and **resultant** electromagnetic forces and torques by applying different kinds of infinitesimal **virtual test velocity fields**.

Nodal forces are obtained by means of a virtual test velocity field leaving all nodes of the mesh but one fixed whereas **resultant forces** are obtained by means of a virtual test velocity field describing an infinitesimal rigid-body motion of the piece under consideration and leaving all other nodes of the mesh fixed.

II. ELECTROMECHANICAL STRESS TENSOR

An important mathematical concept behind the theoretical definition of electromagnetic forces is that of **co-moving time derivative** \mathcal{L}_v . This operator computes the variation in time of a quantity α taking into the fact that the underlying domain of definition is in motion, i.e. the operator that fulfills

$$\partial_t \int_{\Omega} \alpha \, d\Omega = \int_{\Omega} \mathcal{L}_v \alpha \, d\Omega. \quad (1)$$

where the motion is represented by the velocity field \mathbf{v} , which can be virtual or not. According to the geometrical nature of the derived quantity, the co-moving time derivative has the following expression

$$\mathcal{L}_v f = \dot{f} \quad (2)$$

$$\mathcal{L}_v \mathbf{h} = \dot{\mathbf{h}} + (\nabla \mathbf{v}) \cdot \mathbf{h} \quad (3)$$

$$\mathcal{L}_v \mathbf{b} = \dot{\mathbf{b}} - \mathbf{b} \cdot (\nabla \mathbf{v}) + \mathbf{b} \, \text{tr}(\nabla \mathbf{v}) \quad (4)$$

$$\mathcal{L}_v \rho = \dot{\rho} + \text{tr}(\nabla \mathbf{v}) \, \rho \quad (5)$$

where

$$\dot{\mathbf{z}} \equiv \partial_t \mathbf{z} + \mathbf{v} \cdot \nabla \mathbf{z} \quad (6)$$

denotes the *total derivative* of $\mathbf{z}(t, x^k)$, applied component by component to the vector field \mathbf{z} , with respectively (2) for the 0-forms (e.g. temperature), (3) for the 1-forms (e.g. the

magnetic field, or the vector potential), (4) for the 2-forms (e.g. the induction field or the current density), (5) for the 3-forms, which are all volume densities (e.g. the magnetic energy density). Whereas (2) and (5) are classical in fluid dynamics with Eulerian coordinates, their counterpart for vector fields, (3) and (4), which are less often encountered in the literature, are the ones one needs for the analysis of the electromechanical coupling and the definition of electromagnetic forces and torques.

The theoretical definition of electromagnetic forces follows from the evaluation of the co-moving time derivative of the energy density ρ^Ψ considering only the dependency in \mathbf{b} , i.e.

$$\begin{aligned} \mathcal{L}_v \{\rho^\Psi(\mathbf{b})\} &= \dot{\rho}^\Psi(\mathbf{b}) + \text{tr}(\nabla \mathbf{v}) \, \rho^\Psi(\mathbf{b}) \\ &= \partial_{\mathbf{b}} \rho^\Psi(\mathbf{b}) \cdot \dot{\mathbf{b}} + \text{tr}(\nabla \mathbf{v}) \, \rho^\Psi(\mathbf{b}) \\ &= \tilde{\mathbf{h}} \cdot \mathcal{L}_v \mathbf{b} + \{\mathbf{b} \cdot \nabla \mathbf{v} \cdot \tilde{\mathbf{h}} - \text{tr}(\nabla \mathbf{v}) \, \{\tilde{\mathbf{h}} \cdot \mathbf{b} - \rho^\Psi(\mathbf{b})\}\}. \end{aligned} \quad (7)$$

by applying successively (5), (6) and (4). The first term at the r.h.s of (7) is the **variation of the magnetic energy stored in the \mathbf{b} field**. It contains the **magnetic field** $\tilde{\mathbf{h}} \equiv \partial_{\mathbf{b}} \rho^\Psi(\mathbf{b})$, defined as the energy dual of the induction \mathbf{b} . With no motion, $\mathbf{v} = 0 \Rightarrow \mathcal{L}_v = \partial_t$, and the usual definition $\tilde{\mathbf{h}} \cdot \partial_t \mathbf{b}$ is recovered.

By factorizing now $\nabla \mathbf{v}$ in the second term, (7) can be rewritten

$$\mathcal{L}_v \{\rho^\Psi\} = \tilde{\mathbf{h}} \cdot \mathcal{L}_v \mathbf{b} - \rho_{em}^{\dot{W}} \quad (8)$$

with

$$\rho_{em}^{\dot{W}} = -\sigma_{em} : \nabla \mathbf{v} \quad (9)$$

the **work delivered by the magnetic forces** and

$$\sigma_{em} = \mathbf{b} \, \tilde{\mathbf{h}} - \{\tilde{\mathbf{h}} \cdot \mathbf{b} - \rho^\Psi(\mathbf{b})\} \mathbb{I}. \quad (10)$$

the definition of an **electromechanical stress tensor**. Note the use of the dyadic (undotted) vector product $(\mathbf{v} \, \mathbf{w})_{ij} = v^i w^j$, the tensor product $a : b = a_{ij} b_{ij}$ and the identity matrix \mathbb{I} . The electromechanical stress tensor of empty space (or air) is called **Maxwell stress tensor**.

III. ELECTROMAGNETIC FORCES

In this section, it is shown that the variety of methods and formulae to calculate the electromagnetic forces can all be systematically derived from (9) by considering different virtual velocity fields \mathbf{v} .

a) electromechanical stress tensor: We have shown that electromechanical coupling arises from the power delivered by a stress tensor σ_{em} on the gradient of a (virtual) velocity field \mathbf{v} . Indeed, the material derivatives of the p -forms (2)–(5) involve $\nabla\mathbf{v}$, but *not* \mathbf{v} itself. It is thus correct to consider the electromechanical tensor σ_{em} as a fundamental quantity and the electromagnetic forces as a derived quantity (See *c*) below).

b) energy density: The electromechanical properties of a given material are completely determined by the expression of its energy density ρ^Ψ as a function of electromagnetic state variables (the induction \mathbf{b} and the displacement current \mathbf{d}) and the strain ε . Each material has thus its own electromechanical stress tensor σ_{em} , which is derived from this particular expression of the energy density functional by the procedure (7).

Considering for instance a material whose energy density depends on both \mathbf{b} and \mathbf{d} (the empty space is already such a medium), one finds

$$\sigma_{em} = \mathbf{d} \tilde{\mathbf{e}} + \mathbf{b} \tilde{\mathbf{h}} - \{\tilde{\mathbf{e}} \cdot \mathbf{d} + \tilde{\mathbf{h}} \cdot \mathbf{b} - \rho^\Psi(\mathbf{d}, \mathbf{b})\} \mathbb{I}. \quad (11)$$

The energy density of a **magnetostrictive material**, on the other hand, does not depend on \mathbf{d} but has a term depending on both \mathbf{b} and ε . The corresponding electromechanical stress tensor has one extra term

$$\sigma_{em} = \mathbf{b} \tilde{\mathbf{h}} + \partial_\varepsilon \rho^\Psi(\mathbf{b}, \varepsilon) - (\tilde{\mathbf{h}} \cdot \mathbf{b} - \rho^\Psi) \mathbb{I}. \quad (12)$$

Other examples can be found in [7].

c) force density:

The link between the electromechanical stress tensor σ_{em} and the electromagnetic force density $\rho_{em}^{\mathbf{f}}$ is found by making an integration by part of (9) over an arbitrary region Ω :

$$\int_{\Omega} \sigma_{em} : \nabla \mathbf{v} \, d\Omega = - \int_{\Omega} \rho_{em}^{\mathbf{f}} \cdot \mathbf{v} \, d\Omega + \int_{\partial\Omega} \mathbf{n} \cdot \sigma_{em} \cdot \mathbf{v} \, d\partial\Omega \quad (13)$$

with $\rho_{em}^{\mathbf{f}} = \text{div} \sigma_{em}$ by definition and \mathbf{n} the exterior normal to the boundary $\partial\Omega$ of the domain Ω . The power delivered by the electromechanical stress is thus equivalent to the power delivered by a volume density of forces *plus* the power flow delivered by the electromechanical tensor on the boundary of the considered domain.

Making use of the Vector analysis formula

$$-a^i \frac{\partial b^k}{\partial x^i} + a^i \frac{\partial b^i}{\partial x^k} = (\mathbf{a} \times \text{curl} \mathbf{b})^k, \quad (14)$$

the force density derived from (11) is

$$\rho_{em}^{\mathbf{f}} = \text{curl} \tilde{\mathbf{e}} \times \mathbf{d} + \text{curl} \tilde{\mathbf{h}} \times \mathbf{b} + \tilde{\mathbf{e}} \text{div} \mathbf{d} + \tilde{\mathbf{h}} \text{div} \mathbf{b}, \quad (15)$$

and substituting Maxwell equations gives

$$\rho_{em}^{\mathbf{f}} = -\mathcal{L}_{\mathbf{v}}\{\mathbf{b} \times \mathbf{d}\} + \mathbf{j} \times \mathbf{b} + \tilde{\mathbf{e}} \text{div} \mathbf{d} + \tilde{\mathbf{h}} \text{div} \mathbf{b}, \quad (16)$$

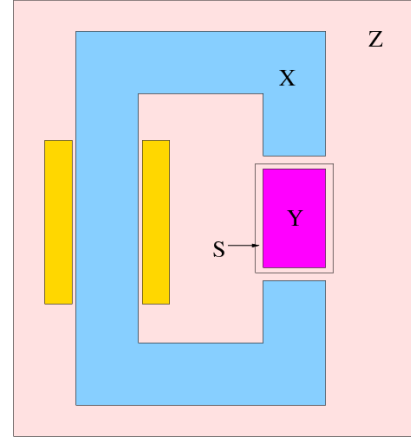


Fig. 1. Canonical electromagnetic force problem, where Y is a moving rigid region (body), Z is a force-free region, X is fixed, S is the eggshell.

where one recognizes the co-moving time variation of the **electromagnetic momentum** $\mathbf{b} \times \mathbf{d}$, the **Lorentz force** and the **electrostatic force**.

d) sign convention: The electromechanical stress tensor σ_{em} is a true mechanical stress, i.e. its work is delivered by the mechanical compartment and received by the electromagnetic compartment. On the other hand, $\rho_{em}^{\mathbf{f}}$ is a magnetic force. Its work is withdrawn from the electromagnetic compartment and received by the mechanical compartment. Hence the minus sign in (9).

e) continuity: The electromechanical stress tensor is in general discontinuous across material interfaces. The jump $\Delta\sigma_{em} \cdot \mathbf{n}_\Sigma$ across a surface Σ is a surface force density. It is easy to check that it is always perpendicular to Σ , so that it can be called **electromagnetic pressure**. The jump operator is also the divergence in the sense of distributions, as can be seen by applying (13) domain by domain, and then summing up the surface contribution on all interfaces.

f) structural mechanics: The electromechanical stress tensor can be used directly as an applied stress in the structural equations and boundary conditions of the system. One has

$$\text{div} \{\sigma + \sigma_{em}\} + \rho^{\mathbf{f}} = 0. \quad (17)$$

When coupling through the forces, on the other hand, $\text{div} \sigma + \{\rho_{em}^{\mathbf{f}} + \rho^{\mathbf{f}}\} = 0$ one has to make sure that the additional condition $\Delta\sigma \cdot \mathbf{n} = \Delta\sigma_{em} \cdot \mathbf{n}$ is also fulfilled across all interfaces.

g) force-free region: The velocity field \mathbf{v} is clearly identified with the tangent vector to the trajectories of material particles at all points in the material regions of the problem. In non-materials regions however (e.g. air), \mathbf{v} is somewhat undetermined. Applying (13) to a force-free region Z , i.e. a region where $\rho_{em}^{\mathbf{f}} = 0$, yields

$$- \int_Z \rho_{em}^{\mathbf{W}} \, dZ = \int_{\partial Z} \mathbf{n} \cdot \sigma_{em} \cdot \mathbf{v} \, d\partial Z. \quad (18)$$

This shows that the velocity field \mathbf{v} is actually arbitrary on the *interior* of Z in the sense that it does not affect

the mechanical power exchanged with that region, which is completely determined by the value of \mathbf{v} on the boundary ∂Z . In all cases, \mathbf{v} must however remain continuous everywhere.

h) rigid region: Let the rigid body motion of a region Y be described by the velocity field $\mathbf{v} = \mathbf{v}_0 + \mathbf{w}_0 \times \mathbf{r}$. Equation (13) gives

$$\begin{aligned} \int_Y \sigma_{em} : \nabla \mathbf{v} \, dY + \int_Y \rho_{em}^f \cdot \{\mathbf{v}_0 + \mathbf{w}_0 \times \mathbf{r}\} \, dY \\ = \int_{\partial Y} \mathbf{n} \cdot \sigma_{em} \cdot \{\mathbf{v}_0 + \mathbf{w}_0 \times \mathbf{r}\} \, d\partial Y. \end{aligned} \quad (19)$$

The vectors \mathbf{v}_0 and \mathbf{w}_0 being homogeneous over Y , one has $(\nabla \mathbf{v})_{ij} = \epsilon_{ijk}(\mathbf{w}_0)_k$ with ϵ_{ijk} is the Levi-Civita symbol. Identifying the factors of the linearly independent vectors \mathbf{v}_0 and \mathbf{w}_0 , one defines the **resultant electromagnetic force**

$$\mathbf{F}_Y \equiv \int_Y \rho_{em}^f \, dY = \int_{\partial Y} \mathbf{n} \cdot \sigma_{em} \, d\partial Y \quad (20)$$

and the **resultant electromagnetic torque**

$$\mathbf{T}_Y \equiv \int_Y \{\hat{\sigma}_{em} + \mathbf{r} \times \rho_{em}^f\} \, dY = \int_{\partial Y} \mathbf{r} \times (\mathbf{n} \cdot \sigma_{em}) \, d\partial Y \quad (21)$$

acting on the rigid region Y . In (21), $(\hat{\sigma}_{em})_k = \epsilon_{ijk}(\sigma_{em})_{ij}$ is the couple stress, which is zero if σ_{em} is symmetric.

Equations (20) and (21) show that the resultant force \mathbf{F}_Y and the resultant torque \mathbf{T}_Y acting on a rigid region Y can both be evaluated by means of a surface integral on the boundary ∂Y . This classical result implies however a surface integration, which requires a specific implementation in the context of a finite element discretization. Note that the rigid region Y need not be identified with a material body. It may be larger, provided that the extra domain enclosed is force-free.

i) eggshell method: In practice, it is easier to work with volume integrations which are already implemented in the finite element programme. In order to get rid of the surface integration in (20) and (21), one chooses a domain Ω larger than the rigid region Y , i.e. enclosing as well a part of a force-free region (generally air). One chooses then a velocity field that describes a rigid motion of Y , decays smoothly outside Y and vanishes on $\partial\Omega$, i.e

$$\mathbf{v} = \{\mathbf{v}_0 + \mathbf{w}_0 \times \mathbf{r}\}\gamma, \quad (22)$$

where γ is any smooth function whose value is 1 on Y and 0 on $\partial\Omega$. One defines the **eggshell** $S \equiv \Omega - Y$ associated with the rigid movement of Y within Ω ; S is a force-free region. Applying now (18) to S yields successively

$$\begin{aligned} - \int_S \sigma_{em} : \nabla \mathbf{v} \, dS &= - \int_{\partial\Omega - \partial Y} \mathbf{n} \cdot \sigma_{em} \cdot \mathbf{v} \, d\partial S \\ &= - \int_{\partial Y} \mathbf{n} \cdot \sigma_{em} \cdot \{\mathbf{v}_0 + \mathbf{w}_0 \times \mathbf{r}\} \, d\partial Y \\ &= \mathbf{F}_Y \cdot \mathbf{v}_0 + \mathbf{T}_Y \cdot \mathbf{w}_0. \end{aligned}$$

On the other hand, substituting (22) in the l.h.s of the latter equation yields

$$\begin{aligned} \int_S \sigma_{em} : \nabla \mathbf{v} \, dS &= \int_S \nabla \gamma \cdot \sigma_{em} \cdot \{\mathbf{v}_0 + \mathbf{w}_0 \times \mathbf{r}\} \, dS \\ &+ \int_S \hat{\sigma}_{em} \cdot \mathbf{w}_0 \, dS. \end{aligned}$$

and, by identification, the resultant force

$$\mathbf{F}_Y = - \int_S \nabla \gamma \cdot \sigma_{em} \, dS, \quad (23)$$

and the resultant torque

$$\mathbf{T}_Y = - \int_S \{\mathbf{r} \times (\nabla \gamma \cdot \sigma_{em}) + \hat{\sigma}_{em} \gamma\} \, dS, \quad (24)$$

now evaluated by means of a volume integral over the eggshell S , instead of integral over the surface of Y (Compare with (20) and (21)). The couple stress $\hat{\sigma}_{em}$ is zero in practice, and will be disregarded in the following.

The eggshell can be defined explicitly by the user, like in Fig. 1, and γ is then a user-defined analytic function; this is Arkkio's approach (See *j*) below). In practice, it is easier to have the eggshell defined automatically, and to reduce its support to a minimum. This aspect is discussed in the section devoted to the implementation of the eggshell method.

j) Arkkio's method: The torque in 2D electrical rotating machines models can be calculated by considering the velocity field

$$\mathbf{v} = \gamma \mathbf{w}_0 \times \mathbf{r} = \frac{R_o - r}{R_o - R_i} \{w_0 \mathbf{e}_z\} \times \{r \mathbf{e}_r\} \quad (25)$$

defined in cylindrical coordinates in a cylindrical region S contained in the airgap. Let R_o and R_i be the outer and inner radius of S . The function γ is thus 0 on the outer surface and 1 on the inner surface of S , The gradient of the velocity field is

$$\nabla \mathbf{v} = \begin{pmatrix} \partial_r v^r & \frac{1}{r} \partial_\theta v^r \\ r \partial_r (\frac{v^\theta}{r}) & \partial_\theta (\frac{v^\theta}{r}) \end{pmatrix} = \frac{-w_0 r}{R_o - R_i} \mathbf{e}_r \mathbf{e}_\theta, \quad (26)$$

whence by (23), the formula of Arkkio [10]:

$$\mathbf{T}_Y = \frac{\mathbf{e}_z}{R_o - R_i} \int_S r (\sigma_{em})_{r\theta}. \quad (27)$$

k) nodal forces: The virtual displacement of one node N_k of a mesh leaving all other nodes fixed corresponds to the velocity field

$$\mathbf{v} = \mathbf{v}_0 \gamma_k$$

with γ_k the nodal shape function of that node. Substituting into (13) gives

$$- \int_\Omega \nabla \gamma_k : \sigma_{em} \, d\Omega \cdot \mathbf{v}_0 = \int_\Omega \rho_{em}^f \gamma_k \, d\Omega \cdot \mathbf{v}_0 \quad (28)$$

which allows to define the **nodal magnetic force** \mathbf{F}_k acting on the node by

$$\mathbf{F}_k \equiv \int_\Omega \rho_{em}^f \gamma_k \, d\Omega = - \int_\Omega \nabla \gamma_k : \sigma_{em} \, d\Omega. \quad (29)$$

By comparison with (23), one sees that node forces are obtained by applying the eggshell approach around every single node of the FE mesh.

This is **Coulomb's formula** (See [13] for linear materials and [11], [14] for non-linear materials), which is also identical to the formula proposed in [12]. Equation (29) is however more general, as it does not assume any particular form of σ_{em} . In each element in the support ω_k of the shape function

γ_k , the appropriate expression of the electromechanical stress tensor must be used, according to the local material properties.

It is important to note at this stage that the nodal electromagnetic forces \mathbf{F}_k are physical quantities if $\Omega \supset \omega_k$, i.e. if the integration domain contains the whole support of the shape function γ_k . In this case, the nodal forces are physical forces, and they can be used directly as a source term in the structural problem. If the support of $\Omega \not\supset \omega_k$, the nodal force is not physical. Such partial nodal forces will however be used below for the computation of resultant forces and torques on rigid bodies. To avoid confusion, they are noted \mathbf{F}_k^S , with $S \not\supset \omega_k$.

IV. IMPLEMENTATION

In this section, a finite element implementation of the eggshell method is proposed. Having a FE mesh, the virtual velocity field (22) is the sum

$$\mathbf{v} = \sum_{N_k \in Y} \gamma_k (\mathbf{v}_0 + \mathbf{w}_o \times \mathbf{r}_k).$$

Substituting in (23) and (24), yields

$$\mathbf{F}_Y = - \sum_{N_k \in Y} \int_S \nabla \gamma_k \cdot \sigma_{em} dS = \sum_{N_k \in Y} \mathbf{F}_k^S \quad (30)$$

and the resultant torque

$$\mathbf{T}_Y = - \sum_{N_k \in Y} \int_S \mathbf{r}_k \times (\nabla \gamma_k \cdot \sigma_{em}) dS = \sum_{N_k \in Y} \mathbf{r}_k \times \mathbf{F}_k^S, \quad (31)$$

where the nodal forces \mathbf{F}_k^S are complete (physical) if $S \supset \omega_k$.

Only the finite elements of the eggshell S bring a contribution contribute to the resultant force/torque on Y , which is the sum of The nodal forces \mathbf{F}_k^S can therefore be evaluated on S only, with a significant gain in computational time. A natural choice for an automatically generated eggshell region S is to take one layer of finite elements around the rigid region, i.e. all elements outside Y having at least one node on the boundary ∂Y . This alternative method to compute the resultant force on rigid bodies has been proposed in [8] and [9].

TABLE I
CALCULATION OF THE TORQUE WITH VARIOUS CHOICES OF THE EVALUATION DOMAIN S AND THE SUMMATION DOMAIN Y .

	S (EVAL)	#EVAL	Y (SUM)	Force [N]	Err. [%]
1	all	19973	R+M+r	76.78813	0.
2	g	3032	r	-76.78813	0.
3	g	3032	s	76.78813	0.
4	r	2952	g	76.812705	0.032
5	r	2952	R	-76.812705	0.032
6	s	3085	g	-76.8802675	0.120
7	s	3085	S+C	76.1677025	0.808

V. APPLICATION 2D

The flexibility of the eggshell approach relies also on the fact that there exist several equivalent choices for S (EVAL) and Y (SUM) that lead in theory to the same result, which allows comparing accuracies and checking consistency. Fig. 2 shows the cross section of a typical 2D Permanent Magnet

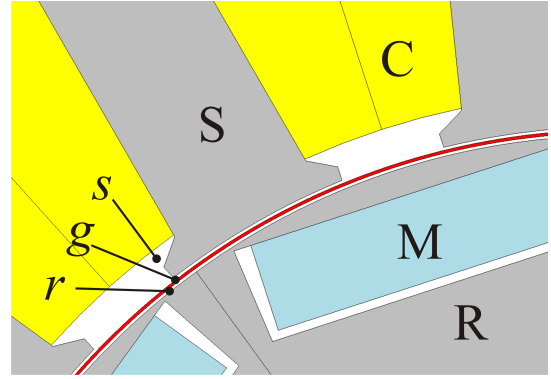


Fig. 2. Cross section of a typical 2D PMSM FE model.

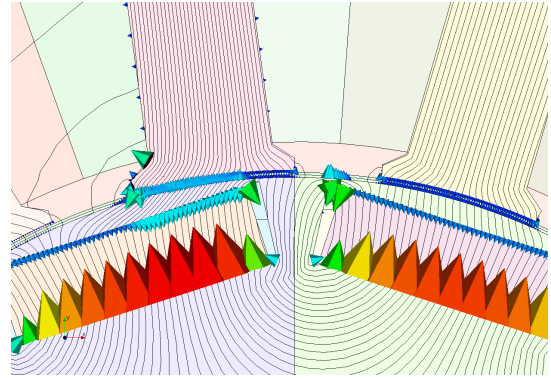


Fig. 3. Nodal magnetic forces computed with S the whole domain occupied by a PMSM machine.

synchronous Machine (PMSM) FE model. The different regions are the stator core S , the rotor core R , the stator coils C and the magnets M . The airgap is divided into three concentric regions, respectively noted s , g and r , from the outermost one (adjacent to the stator) to the innermost one (adjacent to the rotor). The annulus-shaped middle region g , represented in red color, is remeshed at each time step, when using the **moving band method**.

Table I shows the average torque computed with various choices of the evaluation domain S (EVAL) and the summation domain Y (SUM). Line 1 corresponds to the case where the nodal forces have been evaluated at all nodes of the mesh, (S is the whole domain occupied by the machine) and the summation has been done on all rotor nodes (Y is the domain occupied by the rotor as well the airgap region r adjacent to it). The nodal forces are thus physical, and one can see in Fig. 3 that they are, as expected, significant at material discontinuities. There are no forces on the nodes in the air gap. This means that a large number of negligible nodal forces have been uselessly computed in this case. Since nodal forces are net forces (in Newton), and not force densities, larger vectors at the bottom side of the magnets are due to the coarser discretization. This does not necessarily mean that the force density is larger in that region.

Line 2 and Line 3 correspond to the case where nodal forces have been evaluated over the middle airgap region g , i.e. for 3032 nodes instead of 19973 for Line 1. Fig. 4 shows the

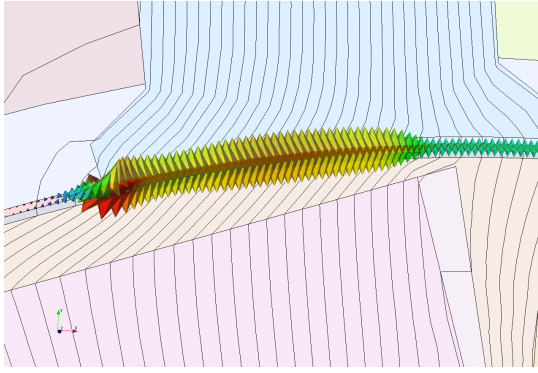


Fig. 4. Nodal forces \mathbf{F}_k^S obtained with $S \equiv g$ a thin annulus-shaped layer of finite elements in the middle of the airgap.

corresponding nodal forces \mathbf{F}_k^g . The computed nodal forces act in opposing direction over the inner and the outer boundaries of the region g . They are not physical, they act at nodes located in air! Only makes sense their algebraic sum to build a resultant force, or the algebraic sum of their respective torque $\mathbf{r}_k \times \mathbf{F}_k$ to build the resultant torque. At Line 2 of the table, the sum is done on the nodes of the region r , i.e. on the nodes of the inner boundary of g , whereas at Line 3 the sum is done on the nodes of s , i.e. on the nodes of the outer boundary of g .

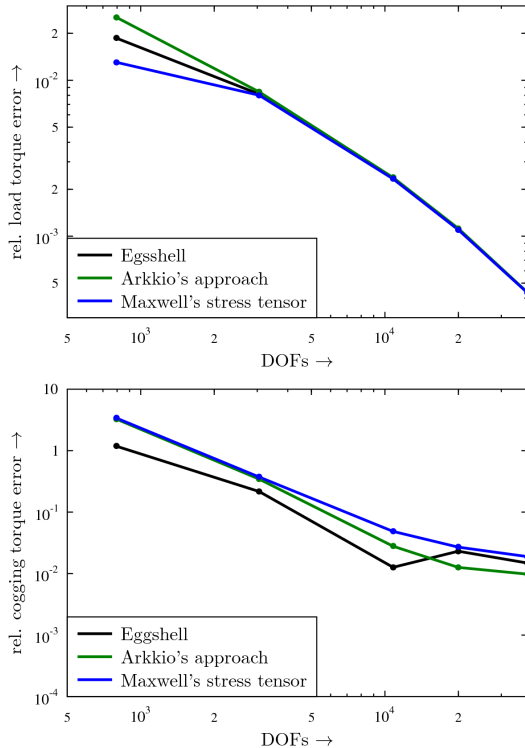


Fig. 5. Convergence analysis of the average torque and the cogging torque.

In the 3 cases so far, the computed torques are identical up to machine precision. Calculation with the surface integration of the Maxwell stress tensor (SIMST [15]) on a surface cylindrical surface in the middle of g , and with Arkkio's method also in the region g give the same value for the

computed torque within a precision of $10^{-3}\%$. The eggshell method is thus able to reproduce the results of those standard methods, with more efficiency than the SIMST (one does not need to slice the mesh) and more generality than Arkkio's method (which is limited to annular regions). The equivalence of the methods applied in the middle of the air gap is confirmed by the convergence analysis of the average torque and the cogging torque in Fig. 5.

The next 4 lines in Table I correspond to other choices of S and Y that should in theory equivalently deliver the same value of the torque. At Line 4 and Line 5, the nodal forces are evaluated in the region r adjacent to the highly saturated bridges over permanent magnets, which yields a decrease of the accuracy. At Line 6 and Line 7, nodal forces are evaluated in regions s with material singularities, with a larger reduction of the accuracy. One sees that the optimal position for an accurate evaluation of the torque is indeed in the middle of the air gap.

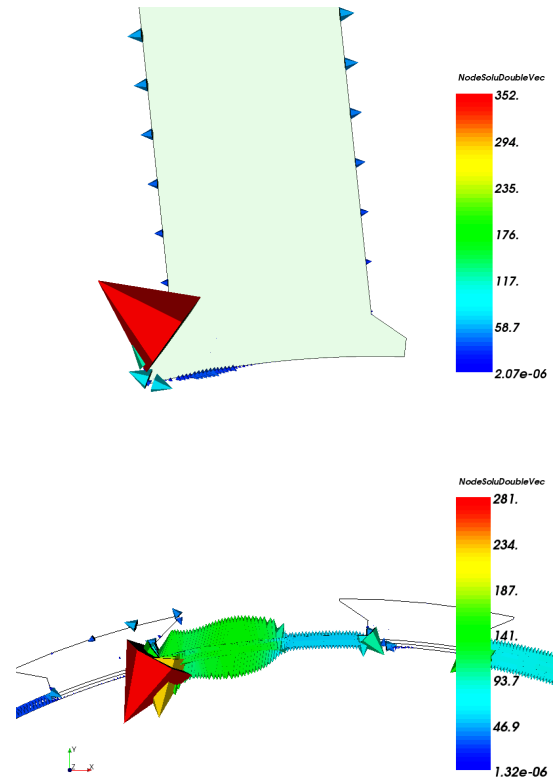


Fig. 6. qq

The eggshell method can be used also to extract additional information about the structure of the force field. Machine designers are interested in the calculation of the efforts on stator teeth for instance. Often, the Maxwell stress tensor (of empty space), or even the magnetic pressure ($\mathbf{b}^2/(2\mu_0)$) are taken as approximation of the electromagnetic forces, disregarding thus the contribution of the electromechanical stress tensor of the steel. Fig. 6 shows the nodal forces \mathbf{F}_k^S with S a stator tooth compared to the nodal forces \mathbf{F}_k^{r+g+s} which represent respectively the internal and the external contribution to the true nodal forces acting on the surface of the tooth. One

can indeed check that the internal contribution is smaller than the external one. It is however far from being negligible in saturated regions.

VI. APPLICATION 3D

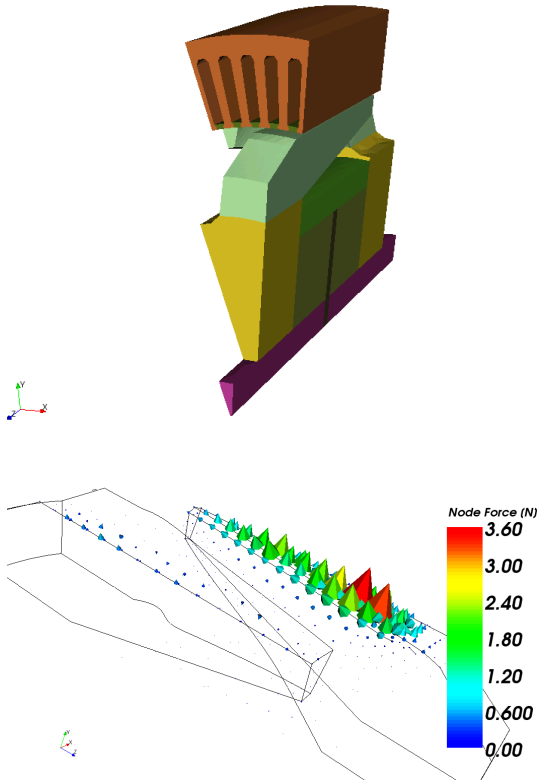


Fig. 7. Geometry of a 30° sector of a clawpole generator, and different views of the nodal forces at the claw surface.

The eggshell method can be applied for the computation of electromagnetic forces and torques in 3D problems as well. Fig. 7 shows the geometry of a 30° sector of a clawpole generator, and different views of the nodal forces at the claw surface.

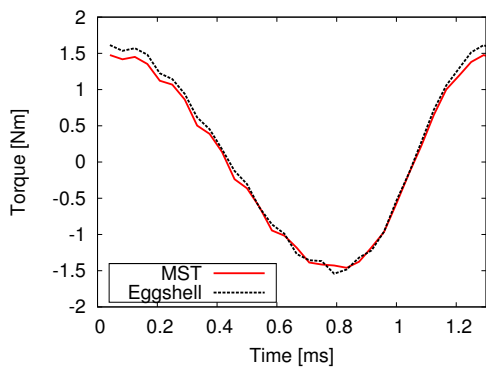


Fig. 8. A comparison between the surface integration of the **Maxwell stress tensor**, with sectioning of the airgap tetrahedrons, and the **eggshell method**.

Fig. 8 shows the comparison between the surface integration of the Maxwell stress tensor, with sectioning of the airgap

tetrahedrons, and the eggshell method. For no slicing of the 3D tetrahedral mesh is required, the computation time of the eggshell method is much smaller.

VII. CONCLUSION

This eggshell method allows computing both local and resultant electromagnetic forces and torques by applying different kinds of infinitesimal virtual test velocity fields. Although the eggshell method can be shown to be equivalent with the Maxwell stress tensor method and with the virtual work principle, it has however a number of practical and conceptual advantages. Contrary to Coulomb's approach, the eggshell method is established at the continuous level, i.e. the theory does not rely on a FE mesh and on discretized fields.

The continuous medium theory behind the eggshell method shows how an electromechanical stress tensor can be uniquely associated with each material, and how this tensor completely represents the electromechanical coupling in that material. The electromechanical stress tensor of empty space is the well-known Maxwell stress tensor. The electromechanical stress tensor of other materials (nonlinear, anisotropic, ...) might however be quite more involved.

REFERENCES

- [1] D.A. Lowther, "Challenges in low frequency electromagnetic analysis and design", In *Proceedings of the 5th IEE international conference on Computational Electromagnetics, CEM'2004*, 19-22 April, Stratford-upon-Avon, UK, pp 1-6.
- [2] A. Bossavit, "Forces inside a magnet", *ICS Newsletter*, ISSN 1026-0854, 11(1):4-12, March 2004.
- [3] A. Bossavit, "Forces in magnetostatics and their computation", *Journal of Applied Physics*, 67(9):5812-5814, 1990.
- [4] A. Bossavit, "Edge element computation of the force field in deformable bodies", *IEEE Transactions on Magnetics*, 28(2):1263-1266, 1992.
- [5] A. Bossavit, "On local computation of the electromagnetic force field in deformable bodies", *International Journal of Applied Electromagnetics in Materials*, 2:333-343, 1992.
- [6] B. Schutz, *Geometrical methods of mathematical Physics*, Cambridge University Press, 1980.
- [7] F. Henrotte, H. Vande Sande, G. Delige, and K. Hameyer, "Electromagnetic force density in a ferromagnetic material", *IEEE Transaction on Magnetics*, 40(2):553-556, March 2004.
- [8] S. McFee, J.P. Webb, and D. Lowther, "A tunable volume integration formulation for force calculation in finite-element based computational magnetostatics", *IEEE Transactions on Magnetics*, 24(1):439-442, 1988.
- [9] F. Henrotte, G. Delige, and K. Hameyer, "The eggshell approach for the computations of electromagnetic forces in 2D and 3D", In *Proceedings of the 6th international symposium on electric and magnetic fields, EMF'2003*, pages 55-58, Aachen (Germany), October 2003.
- [10] A. Arkkio, "Analysis of induction motors based on the numerical solution of the magnetic field and circuit equations", *Acta Polytechnica Scandinavica*, 1987, p. 56.
- [11] J.L. Coulomb, "A methodology for the determination of global electromechanical quantities from a finite element analysis and its application to the evaluation of magnetic forces, torques and stiffness", *IEEE Transactions on Magnetics*, 16(6):2514-2519, 1983.
- [12] A. Kameari, "Local force calculation in 3D FEM with edge elements", *International Journal of Applied Electromagnetics in Materials*, 3:231-240, 1993.
- [13] Z. Ren and A. Razek, "Local force computation in deformable bodies using edge elements", *IEEE Transactions on Magnetics*, 28(2):1212-1215, 1992.
- [14] Z. Ren, M. Besbes, and S. Boukhtache, "Calculation of local magnetic forces in magnetized materials", In *Proceedings of the 1st International Workshop on Electric and Magnetic Fields*, Lige (Belgique), September 1992.
- [15] J.R. Melcher, *Continuum electromechanics*. The MIT Press, 1981.
- [16] H.H. Woodson and J.R. Melcher, *Electromechanical dynamics I, II and III*, John Wiley, 1968.